

6-1-1983

A Study of the 0.1-EV Conversion Acceptor in GaAs

David C. Look

Wright State University - Main Campus, david.look@wright.edu

Gernot S. Pomrenke

Follow this and additional works at: <http://corescholar.libraries.wright.edu/physics>



Part of the [Physics Commons](#)

Repository Citation

Look, D. C., & Pomrenke, G. S. (1983). A Study of the 0.1-EV Conversion Acceptor in GaAs. *Journal of Applied Physics*, 54 (6), 3249-3254.

<http://corescholar.libraries.wright.edu/physics/103>

This Article is brought to you for free and open access by the Physics at CORE Scholar. It has been accepted for inclusion in Physics Faculty Publications by an authorized administrator of CORE Scholar. For more information, please contact corescholar@www.libraries.wright.edu.

A study of the 0.1-eV conversion acceptor in GaAs

D. C. Look

University Research Center, Wright State University, Dayton, Ohio 45435

Gernot S. Pomrenke

Avionics Laboratory, Wright-Patterson Air Force Base, Ohio 45433

(Received 16 August 1982; accepted for publication 1 February 1983)

Two semi-insulating liquid-encapsulated Czochralski GaAs crystals, one Cr-doped and the other undoped, were annealed at 750 °C for 15 min in flowing H₂. Each sample converted to conducting *p* type in the near-surface region, due to the formation of acceptors at $E_v + 0.1$ eV. We have studied this phenomenon by electrical, optical, and analytical profiling techniques, and have determined conclusively that the acceptors in our samples are *not* related to Mn accumulation, a commonly accepted explanation. It is argued that the 0.1-eV center may arise from several possible sources, each exhibiting a V_{Ga} -like state at this energy.

PACS numbers: 72.80.Ey, 71.55.Fr, 72.20.My

I. INTRODUCTION

The existence of a semi-insulating (SI) form of GaAs has been essential for the development of much of the present-day GaAs device technology.¹ A well-known problem with SI GaAs, however, is the "conversion" phenomenon, in which a thin, conducting surface layer is formed upon heating to the temperatures required for epitaxial growth, or ion-implantation annealing. One of the most common types of conversion involves a *p*-type layer which exhibits a thermal (Hall-effect) activation energy of 0.1 eV, and a photoluminescence line at 1.41 eV. Such a layer is formed, e.g., by annealing SI GaAs in H₂ gas at 700–800 °C. The relevant acceptor has been attributed to Mn_{Ga} ,²⁻⁷ $Si_{As} - V_{As}$,⁸⁻¹¹ $C_{As} - V_{As}$,¹⁰⁻¹² and V_{As} .¹³ In an attempt to study this problem further, Yu and Park⁴ have compared the shapes and temperature dependences of the respective 1.41-eV emission lines from Mn-implanted samples, and unimplanted, annealed SI samples. The results were nearly identical. Thus, we feel that Mn_{Ga} represents the most likely cause of the 1.41-eV emission in the majority of annealed samples investigated to date, although the other possibilities, mentioned above, cannot be ruled out in all cases.

We report here a rather extensive investigation of two semi-insulating liquid-encapsulated Czochralski crystals, one undoped (sample F) and the other Cr doped (sample G). Both samples were annealed at 750 °C, face up, for 15 min in an H₂ ambient, to simulate vapor-phase epitaxial (VPE) growth conditions. The surfaces appeared unchanged after the anneals. This treatment produced, in each case, a *p*-type

layer with a sheet resistivity of about $10^5 \Omega/\square$, due to a dominant acceptor level about 0.1 eV from the valence band. Also, a 1.41-eV emission line was observed. However, we will show that the acceptor is definitely not related to Mn, even though the 1.41-eV emission probably is. Thus, the elimination of Mn from the substrate and growth ambient will not eliminate conversion, at least not in all cases. Indeed, it appears that a defectlike state may be the most important constituent of the 0.1-eV center.

In this paper we will present and compare electrical profiles, as determined by differential-Hall (DH) and temperature-dependent Hall (TDH) measurements, and Mn profiles, as determined by photoluminescence (PL) and secondary-ion mass spectroscopy (SIMS) data. Some of the DH, TDH, and SIMS results were presented earlier, in brief form.¹⁴ However, the PL profiles of the 1.41-eV line add a strong confirmation to the basic correctness of the SIMS Mn profiles, and thus to the validity of our conclusions regarding the role of Mn in the conversion process.

II. ELECTRICAL MEASUREMENTS

Room-temperature electrical characteristics for unannealed and annealed crystals are shown in Table I. It is apparent that both samples converted from *n* type, with initial sheet resistivities of about $10^9 \Omega/\square$, to *p* type, with final sheet resistivities of about $10^5 \Omega/\square$. Temperature-dependent Hall-effect data are shown in Fig. 1. They were fitted to the following simple charge-balance equation¹⁵:

TABLE I. Electrical measurement data on samples F and G, before and after a 750 °C, 15-min anneal. The symbol p_s denotes the average hole concentration in the surface (converted) region.

Sample	Anneal	Type	$\rho(\Omega/\square)$	$\mu\left(\frac{\text{cm}^2}{\text{V sec}}\right)$	$n_{\square}(\text{or } p_{\square})(\text{cm}^{-2})$	Minimum		
						$p_s(\text{cm}^{-3})$	$N_A(\text{cm}^{-3})$	$N_{DS} - N_{AS}(\text{cm}^{-3})$
F	None	<i>n</i>	9.8×10^8	2.9×10^3	2.2×10^6			
	750 °C	<i>p</i>	1.0×10^5	2.0×10^2	3.0×10^{11}	4×10^{16}	3×10^{17}	2×10^{17}
G	None	<i>n</i>	3.5×10^9	6.2×10^2	2.8×10^6			
	750 °C	<i>p</i>	7.1×10^4	1.4×10^2	6.3×10^{11}	5×10^{16}	2×10^{17}	6×10^{16}

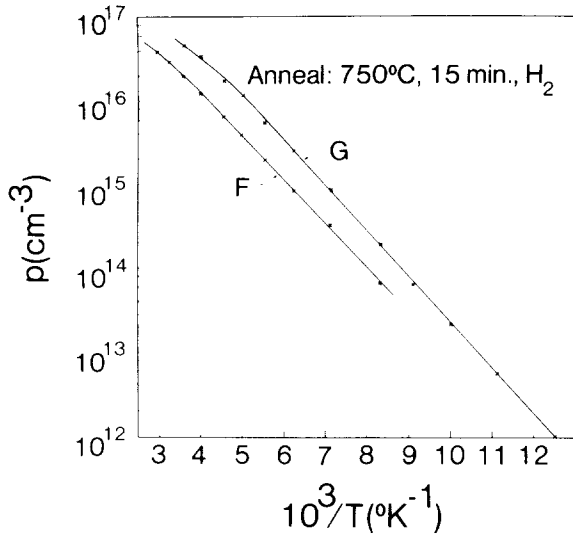


FIG. 1. The hole concentrations vs inverse temperature for samples F and G after an anneal of 750 °C for 15 min in H₂. The solid lines are theoretical fits of Eqs. (1) and (2), in the text, with the following parameters: sample F: $N_A = 3.4 \times 10^{17} \text{ cm}^{-3}$, $N_{DS} - N_{AS} = 2.3 \times 10^{17} \text{ cm}^{-3}$, $E_A = 0.085 \text{ eV}$, and $C = 4.1 \times 10^{14} \text{ cm}^{-3} \text{ K}^{-3/2}$; sample G: $N_A = 2.3 \times 10^{17} \text{ cm}^{-3}$, $N_{DS} - N_{AS} = 5.9 \times 10^{16} \text{ cm}^{-3}$, $E_A = 0.094 \text{ eV}$, and $C = 4.1 \times 10^{14} \text{ cm}^{-3} \text{ K}^{-3/2}$. Here the value of C was fixed by letting $g_0 = 4$, $g_1 = 1$, and $\alpha = 0$.

$$n + N_{AS} + \frac{N_A}{1 + p/\phi_A} = p + N_{DS}, \quad (1)$$

where $p(n)$ is the free-hole (electron) concentration, N_A is the conversion acceptor concentration, $N_{DS}(N_{AS})$ is the concentration of all donors (acceptors) lying more than a few kT above (below) the Fermi energy, and

$$\phi_A = (g_1/g_0)e^{\alpha/k} N_v' T^{3/2} e^{-E_{A0}/kT} \equiv CT^{3/2} e^{-E_{A0}/kT}, \quad (2)$$

where $g_1(g_0)$ is the degeneracy of the occupied (unoccupied) conversion acceptor state, $N_v' T^{3/2}$ is the valence-band effective density of states, E_{A0} is the ionization energy of the conversion acceptor at $T = 0$, and α is defined by $E_A = E_{A0} - \alpha T$.

To apply Eqs. (1) and (2) it is necessary to know the electrical thickness of the covered layer. That is, dealing with *sheet* concentrations only is insufficient here because of the p/ϕ_A term in Eq. (1), where ϕ_A is in units of cm^{-3} . The electrical thicknesses were obtained from the free-hole profiles, as determined by differential-Hall-effect (DH) data, shown in Fig. 2. (Note that the hole concentrations are multiplied by scale factors, as explained in the Fig. 2 caption.) The *surface* depletion widths for each sample were calculated by assuming a Fermi-level pinning at $E_v + 0.5 \text{ eV}$, the accepted value for *p*-type GaAs. The *interface* depletion widths could not be determined accurately, since the energies and densities of the dominant traps in the respective substrates were not known. Estimates of d_i range from 100 to 1000 Å, depending on the relative sizes of N_T and $[N_A - (N_{DS} - N_{AS})]$.¹⁶ (For illustrative purposes, in Fig. 2, the larger values of d_i are chosen for each sample.) In any case, the hole concentrations in the *conductive* regions were flat, within error, and the thickness of these regions are not expected to vary strongly with temperature, since the deple-

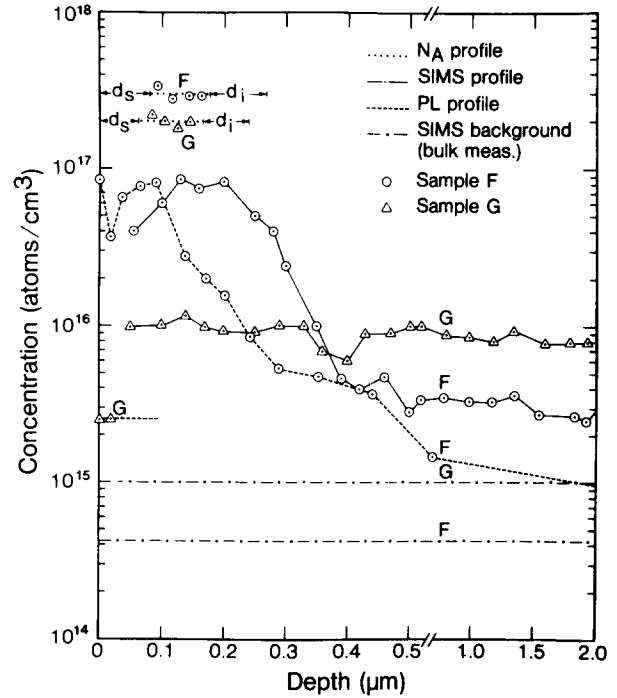


FIG. 2. Profiles of the free-hole concentrations (from DH data), the 0.1-eV acceptor concentrations (from TDH data), the Mn concentrations (from SIMS data), and the 1.41-eV emission (from PL data) in samples F and G, annealed at 750 °C for 15 min in flowing H₂. The free-hole concentrations for samples F and G (denoted by raw data around the N_A profiles) have been multiplied by factors of 7 and 4, respectively, in order to show their relationships to the N_A concentrations, and also to avoid interference with the PL and SIMS profiles. The symbols d_s and d_i denote estimated surface and interface depletion widths, respectively. The PL data, for both samples, are normalized by setting the PL peak voltage for sample F equal to the SIMS peak concentration for sample F. Also shown are *bulk* SIMS data for the *unannealed* samples. Note the x-axis scale change at 0.5 μm.

tion widths themselves are relatively insensitive to temperature. Thus, the TDH data for each sample could be reliably fitted by assuming a flat profile within an electrical thickness of about 0.1 μm.

The four parameters determined from fitting Eqs. (1) and (2) are N_A , $N_{DS} - N_{AS}$, E_{A0} , and $(g_1/g_0) \exp(\alpha/k)$. Unfortunately, because of the lack of high-temperature data, the exhaustion region could not be clearly defined, and therefore only E_{A0} could be determined with precision. (The influence of substrate conduction obscured the higher temperature results.) Thus, for the fits shown in Fig. 1 we fixed $(g_1/g_0) \exp(\alpha/k) = 1/4$, the commonly assumed value for valence-band-like acceptors¹⁵ (i.e., $g_0 = 4$, $g_1 = 1$, $\alpha = 0$), and let the other parameters vary. These fits gave $N_A \approx 3 \times 10^{17} \text{ cm}^{-3}$ for sample F, and $2 \times 10^{17} \text{ cm}^{-3}$ for sample G. However, from the point of view of this study, it is more important to know the *minimum* values of N_A which can still provide reasonable fits to the two sets of data. It turns out that the values mentioned above (and in Fig. 1) are quite close to the minimum values. That is, we can obtain fairly good fits with values of N_A somewhat higher than those given here, but not lower. These minimum values of N_A are listed in Table I. Also listed are the values of $(N_{DS} - N_{AS})$ corresponding to the minimum N_A 's. The identity of these

compensating donors is unknown, since no SIMS data were obtained on the shallow impurities. Defects may also be involved.

III. ANALYTICAL MEASUREMENTS

Secondary-ion mass spectrographic (SIMS) *profile* data on the annealed samples, as well as SIMS *bulk* data on the unannealed samples, were obtained from Charles Evans and Associates. No special preparations were carried out before the SIMS measurements. The results are shown in Fig. 2. It is immediately obvious that the background Mn concentrations, as determined from the *bulk* SIMS analyses, are appreciably lower than the respective *apparent* background concentrations, as determined from the SIMS *profile* analyses. The most obvious reason for this discrepancy involves the background flux of Mn coming from the spectrometer itself, perhaps due to stainless-steel components. This fictitious background is minimized at the very high sputtering rates used for *bulk* studies, but may be much more important at the relatively low sputtering rates used for *profile* studies. Thus, the SIMS profile for sample F is accurate only above about 10^{16} cm^{-3} , while the flat SIMS profile for sample G is probably too high along its entire length. The photoluminescence profiles, to be discussed later, confirm this picture. Well above background levels, the SIMS data are considered accurate to within a factor 2.

Spark-source mass spectrographic (SSMS) measurements on the unannealed samples were also obtained, in our laboratory. The SSMS results agree well with the bulk SIMS results (within a factor 2), but it should be remembered that both techniques are operating near their minimum detectabilities for Mn under these conditions. Thus, measured Mn concentrations below 10^{15} cm^{-3} should not be considered accurate, but only an upper limit.

It is also significant to note that four other samples were analyzed by SIMS at the same time as the two discussed in this work, and the Cr profiles for all six were normal in regard to the present understanding of Cr redistribution in heat-treated GaAs. Thus, there is no reason to consider the Mn profiles anomalous in any way.

IV. PHOTOLUMINESCENCE MEASUREMENTS

A zero-phonon emission line near 1.41 eV is an indicator of Mn impurity. By etching successive layers of substrate and probing with an excitation source of very shallow penetration it is possible to obtain information on the 1.41-eV emission as one goes from the surface through the converting layer and beyond. It may be noted that NRL group⁵ carried out a similar experiment, although with a longer-wavelength excitation source (6471 Å).

The luminescence was generated by a multiline ultraviolet (337.5, 350.7, 356.4 nm) laser source which has an averaged absorption constant of $6.84 \times 10^5 \pm 2\% \text{ cm}^{-1}$ or a penetration depth of $146 \pm 2\% \text{ Å}$ at the $1/e$ point. This strong absorption permitted the sampling of luminescence from very shallow regions of the substrate and made possible a comparison of the optical data with both the SIMS and differential Hall measurements. (The effective resolution

would be degraded, of course, if carrier diffusion lengths were much greater than the penetration depth. However, our samples have similar electrical properties to those used by Klein, Nordquist, and Siebenmann⁵ to estimate a diffusion length of about $0.125 \mu\text{m}$, greater than the UV penetration depth.) Beam diameter at the $1/e^2$ point on the sample was approximately 2 mm, resulting in a sample irradiance of $\sim 0.3 \text{ W/cm}^2$. A 3/4-m Czerny-Turner spectrometer was used in conjunction with a S-1-type photomultiplier tube, cooled to -100°C for processing the luminescence. Due to the poor luminescence efficiency of the unannealed sample G, spectrometer slits were chosen for a resolution of 2 meV. Successive layers, varying from 0.018 to $2.0 \mu\text{m}$, were etched off by using a cooled (0.5°C) 1:1:250 solution of $\text{H}_2\text{O}_2\text{:H}_2\text{SO}_4\text{:H}_2\text{O}$, which resulted in an etch rate of $32 \pm 2\% \text{ Å/min}$, as calibrated by a Dektak Microtopographer. Before face-up annealing at 750°C for 15 min in flowing hydrogen, the samples were cleaned with H_2O , basic H, H_2O , trichloroethylene, acetone, methanol, and finally HCl for oxide removal. A selected number of samples were examined for the effects of preanneal etching, which included the use of a 1:1:3 solution of $\text{H}_2\text{O}_2\text{:H}_2\text{SO}_4\text{:H}_2\text{O}$, or a 0.1%-Br-methanol solution.

The photoluminescence spectra of sample F at 4.2°K are shown in Fig. 3 for both the unannealed and annealed states as a function of depth. The following emissions are evident: the 1.513-eV near-edge emission (NE) which is due to excitonic transitions; the residual free-to-bound (FB) and donor-acceptor (DA) transitions at 1.486 eV and their phonon replicas (LO_1 , LO_2) at 1.454 and 1.417 eV, respectively; the manganese 1.408-eV peak and its associated TA (1.398 eV) and LO (1.372 eV) phonons; and the 1.356-eV emission which is assigned to copper.¹⁷ Upon annealing, the 1.408-eV manganese peak and its associated structure become the dominant, low-energy emissions. As seen most dramatically in Fig. 2, as successive layers of material are removed (initially in increments of $\sim 200 \text{ Å}$) there is a near-surface concentration of the Mn emission which begins to drop sharply at about 2000 Å and finally reaches a background level near $4000\text{--}5000 \text{ Å}$. (The PL and SIMS data for sample F are normalized at their respective peaks.) At the background level, which presumably is associated with a Mn ion concentration of $\sim 4 \times 10^{14} \text{ cm}^{-3}$ (as determined by bulk SIMS), evidence of the Mn emission can only be seen as a low-energy tail of the LO_2 emission. Essentially, one can conclude that any significant and detectable concentration of Mn for sample F is in a $3000\text{--}4000\text{-Å}$ layer from the surface. The 1.356-eV copper peak also appears as the material is annealed and its intensity remains relatively constant throughout the profiling, except in the top 3000 Å . As little change occurs in the Cu emission with depth, it is assumed to be of uniform concentration in the annealed substrate. If relative intensities of the emissions other than Mn are plotted against depth there is a general decrease in luminescence in the top 3000-Å layer, and then, as one etches deeper, the intensities become constant. This indicates that there may be a mechanism associated with the appearance of the Mn which suppresses the residual emissions. When compared to each other, the intensity ratios of the FB-DA, LO_1 , and Cu

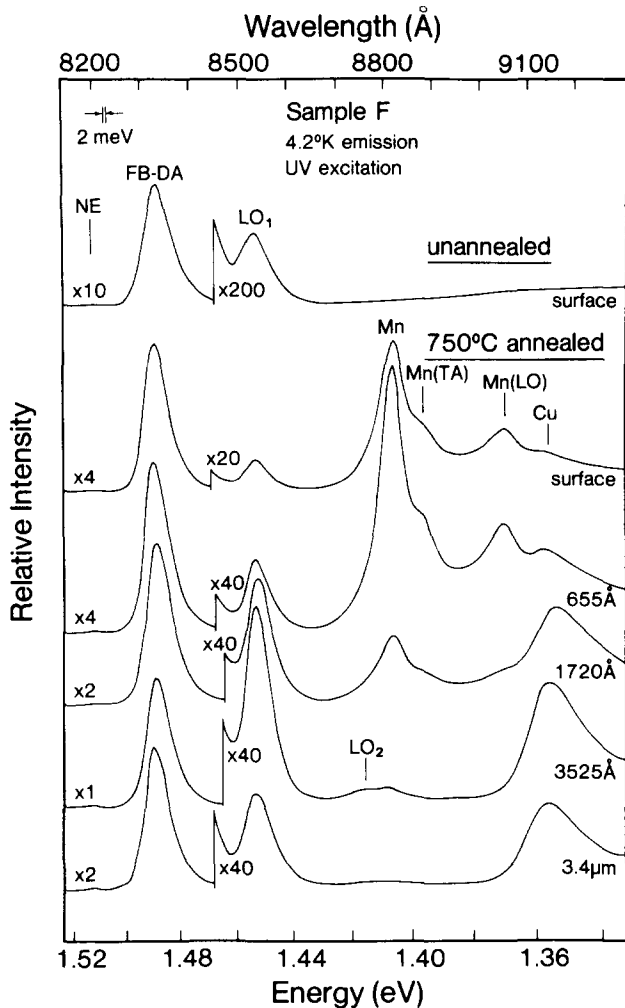


FIG. 3. Luminescence spectra as a function of depth for sample F after a 750 °C anneal. Also shown is the spectrum for sample F before the anneal. Various emission lines are labeled according to presently accepted interpretations.

emissions remain essentially constant from the surface to the deepest etch, indicating that no substantial modification of the material itself occurs upon annealing.

Under the same excitation and temperature conditions, the near-edge emission intensity of unannealed, untreated sample G is about 1/16 of that of sample F. As shown in Fig. 4, after annealing sample G the same impurity emissions develop as in sample F but in a very shallow surface layer and at a much lower intensity. The maximum difference between the Mn peaks of the two samples occurs at the surface where the 1.408-eV peak of sample F is 35 times stronger than that of sample G (cf. Fig. 2). Furthermore, the Mn related peaks disappear somewhere between 190 and 560 Å, the two final etch depths in this particular case. These factors effectively demonstrate the essential absence of manganese as an optically active center in sample G.

In Fig. 2, the PL profile for sample G was plotted by using the same voltage (PL) to concentration (SIMS) ratio as that determined for sample F. (As discussed before, the PL voltage for sample F was normalized to the SIMS concentration for sample F at their respective peaks.) In spite of the possible differences in the two samples regarding factors

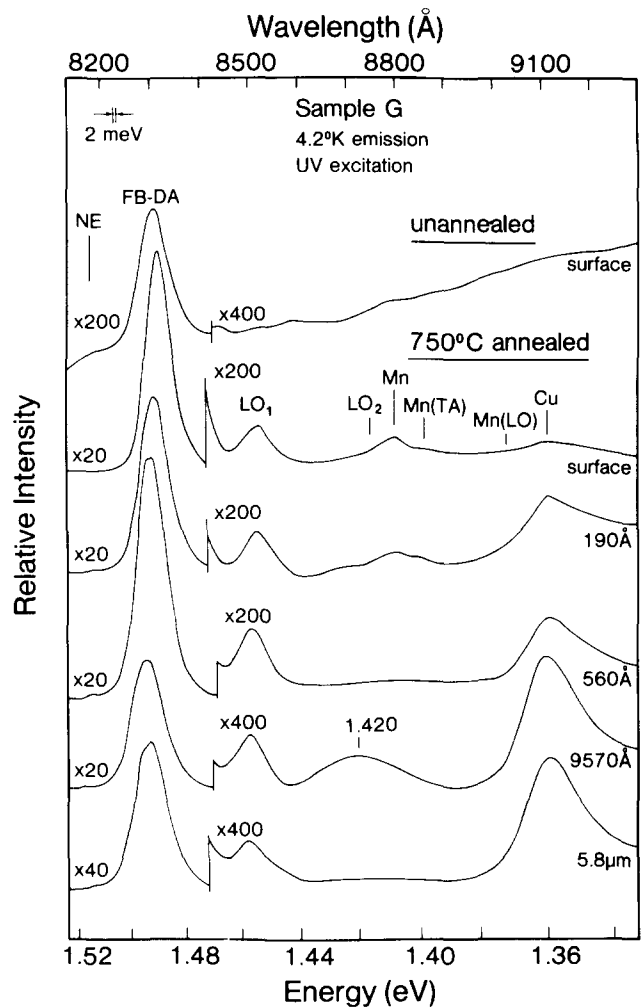


FIG. 4. Luminescence spectra as a function of depth for sample G after a 750 °C anneal. The intensity scale is the same as that used in Fig. 3.

such as radiative efficiency (which might explain the relative FB-DA strengths), it is seen that the Mn concentration for sample G, predicted from the PL data, falls within a factor 2 of the Mn concentration as determined from the bulk SIMS results. Thus, the overall agreement between the SIMS and PL profiles is reasonably good. It may be noted that for sample F the SIMS profile seems somewhat shifted to the right with respect to the PL profile. Although the reasons for this difference are not fully understood, it appears that the origin for the SIMS data should probably be shifted about 500 Å to the left. Also, carrier diffusion effects could shift the PL curve to the right.

As in sample F, the Cu peak in sample G remains relatively constant from the surface to the maximum depth of 7 μm. It is also interesting to note the development of a broad (48 meV, half-width at half maximum), low-intensity peak at 1.420 eV between the depth of 0.5 and 2.3 μm. This energy position has previously been assigned to the $V_{As}-Si_{As}$ complex.^{8,9} However, we will discuss this center further in Sec. V.

In the course of this investigation it was also found that strong preetches (0.5- to 14-μm layer removal) can affect the

surface Mn peak. Sample G was chosen for a detailed study, due to its small *bulk* Mn peak. Three preanneal experiments were performed, one using a 1 H₂O₂:1 H₂SO₄:3 H₂O solution, another using a 0.1%-Br-methanol mixture, and finally one with a solution of undiluted HCl. All three etchants enhanced the Mn peak once the samples were annealed, but the most substantial change occurred when Br-methanol was used to remove a 14- μm layer; the Mn signal was stronger by a factor of 10 as compared to the signal in the absence of preanneal treatment. Most importantly, when a 370- \AA layer was etched off the annealed material, the Mn peak essentially disappeared. The near-surface concentration may be due to the preferential etch of the GaAs versus other impurities, in the material, such as Mn. Then, as the GaAs is removed, trace amounts of Mn from the bulk are left behind which are finally moved into optically active sites upon annealing. Thus, the small Mn surface peak in sample G (Fig. 4) may result from the manufacturer's final etch rather than from diffusion during annealing. In any case, the Mn from this effect disappeared within 500 \AA .

V. DISCUSSION

From the reasonable agreement between the PL and SIMS results, in Fig. 2, it appears that we understand the behavior of Mn in our two, annealed samples. The comparison with the DH and TDH results then leaves no doubt that the concentration of the 0.1-eV acceptor is much greater than the Mn concentration in the converted region, in fact, a factor 20 for sample C. (This factor is probably even greater, due to the SIMS background problems, as discussed earlier.) Thus, we have conclusively demonstrated that Mn is not always the cause of the 0.1-eV acceptor. In some cases, of course, Mn may be responsible, and indeed, may contribute about 20% of the acceptors in sample F. However, we must search for a more general explanation of the 0.1-eV acceptor, and some speculations on this matter are given below. We will attempt to establish that the 0.1-eV level basically stems from a defect state.

First, it is known that a point defect at $E_v + 0.1\text{eV}$ is produced by high-energy (e.g., 1-meV) electrons.¹⁸ Although the exact identity of this defect is unknown, it is stable at room temperature, and thus is probably not an interstitial but either a vacancy or an antisite. Much recent theoretical work on vacancy energy levels has been carried out, and there is general agreement that the arsenic vacancy is in the upper one-quarter of the GaAs band gap,¹⁹⁻²⁶ and the gallium vacancy is in the lower one-third.¹⁹⁻²⁸ Only a few theoretical papers have been written on the antisite defects, but it appears that As_{Ga} (Refs. 26 and 27) is in the upper part of the gap, and Ga_{As}, in the lower part.²⁶ From these arguments, it seems that the point defect at $E_v + 0.1\text{eV}$, created by electron irradiation, would most likely be either V_{Ga} or Ga_{As}. However, our *conversion* center could not be *identical* to any point defect, because *all* of the electrically-active point defects created by 1 MeV electrons are unstable above 300 °C.²⁹ Nevertheless, there are defect *complexes* expected to exhibit a state close to the unfilled V_{Ga} t_2 state. Two of these are V_{Ga} V_{As} (Refs. 24 and 30) and V_{Ga} Ga_{As},²⁶ both quite probable because of expected V_{Ga} and V_{As} in-diffusion during the

anneal.^{2,3,5} Another is V_{Ga}-*D*, where *D* is a neighboring donor impurity. (In ZnSe it has been found that several V_{Zn}-*D* gap levels are close to the V_{Zn} gap level.³¹) Also, V_{Ga} clusters might be expected to have levels near the single V_{Ga} t_2 state. In Si, e.g., the theoretical energy of an isolated vacancy level in the band gap is found to be altered very little by pairing with a second point defect.³²

How then would Mn fit into this picture, since it is well known that Mn forms a 0.1-eV acceptor, and the sharpness of the 1.41-eV PL line suggests that it is a simple substitutional, i.e., Mn_{Ga}. The answer may again come from theoretical results. Hemstreet²⁸ has carried out cluster calculations of transition-metal impurities in a GaAs host and finds that Ni and Cu on the Ga site exhibit a state quite like that of the isolated V_{Ga}. Fazio, Leite, and De Siqueira have come to the same conclusion for Cu_{Ga}.²⁰ The theoretical results for Mn are somewhat uncertain because of the strong multi-electron effects expected for a half-filled shell.²⁸ *Experimentally*, however, Ni, Cu, Mn, and Co all exhibit acceptor levels between $E_v + 0.1\text{eV}$ and $E_v + 0.2\text{eV}$.³³ Thus, Mn and Co, as well as Ni and Cu may have a state not too highly perturbed from the V_{Ga} t_2 gap state.

The evidence presented above seems to indicate that there may be several potential sources of the 0.1-eV conversion level, with *all* of them exhibiting a basic, V_{Ga}-like state. One of the elements of this picture is that the $E_v + 0.1\text{eV}$ point defect is indeed a t_2 state of V_{Ga}, an identification which is new, to our knowledge. Another element, technological in nature, is that one way to suppress the conversion phenomenon might be to suppress the Ga vacancy concentration during the anneal. Further evidence on these matters should be sought.

As mentioned earlier, the 1.42-eV PL line, appearing in Fig. 4, has previously been assigned to V_{As}-Si_{As}.⁸ While this assignment may be correct, it is tempting, in light of the energy proximity to the centers discussed above, to suggest that a connection to V_{Ga} may be more appropriate. In either case, it is not clear why this center appears only in a confined region, 0.5–2 μm below the surface.

VI. CONCLUSIONS

The 0.1-eV acceptor level formed by high-temperature annealing is not *always* due to Mn, although Mn may sometimes be involved. Several other possibilities exist, including V_{Ga}, V_{Ga} V_{As}, V_{Ga} Ga_{As}, V_{Ga}-*D*, V_{Ga} clusters, and other transition metals on the Ga site. The basic element of the picture presented here is that all of these possible species have a state closely related to the V_{Ga} t_2 gap state, which we postulate to exist at $E_v + 0.1\text{eV}$.

ACKNOWLEDGMENTS

We would like to thank P. W. Yu, Y. K. Yeo, and J. E. Ehret for helpful discussions, and T. A. Cooper, C. Geesner, and D. E. Johnson for technical assistance. This work was carried out at the Avionics Laboratory, Wright-Patterson Air Force Base, and partially supported under Contract No. F33615-81-C-1406.

- ¹See, for example, *Semi-Insulating III-V Materials*, edited by G. J. Rees (Shiva, Orpington, U.K., 1980).
- ²J. Hallais, A. Mircea-Roussel, J. P. Farges, and G. Poiblaud, in *Gallium Arsenide and Related Compounds (St. Louis 1976)*, edited by L. F. Eastman (Institute of Physics, London, 1976), p. 220.
- ³R. Zucca, in Ref. 2, p. 228.
- ⁴P. W. Yu and Y. S. Park, *J. Appl. Phys.* **50**, 1097 (1979).
- ⁵P. B. Klein, P. E. R. Nordquist, and P. G. Siebenmann, *J. Appl. Phys.* **51**, 4861 (1980).
- ⁶A. Mircea-Roussel, G. Jacob, and J. P. Hallais, in *Semi-Insulating III-V Materials (Nottingham, 1980)*, edited by G. J. Rees (Shiva, Orpington, U.K. 1980), p. 133.
- ⁷J. B. Clegg, G. B. Scott, J. Hallais, and A. Mircea-Roussel, *J. Appl. Phys.* **52**, 1110 (1981).
- ⁸T. Itoh and M. Takeuchi, *Jpn. J. Appl. Phys.* **16**, 227 (1976).
- ⁹E. V. K. Rao and N. Duhamel, *J. Appl. Phys.* **49**, 3548 (1978).
- ¹⁰W. Y. Lum, H. H. Wieder, W. H. Koschel, S. G. Bishop, and B. D. McCombe, *Appl. Phys. Lett.* **30**, 1 (1977).
- ¹¹W. Y. Lum and H. H. Wieder, *J. Appl. Phys.* **49**, 6187 (1978).
- ¹²W. Y. Lum and H. H. Wieder, *Appl. Phys. Lett.* **31**, 213 (1977).
- ¹³M. Otsubo, H. Miki, and S. Mitsui, *Jpn. J. Appl. Phys.* **16**, 1957 (1977).
- ¹⁴D. C. Look, P. W. Yu, J. E. Ehret, Y. K. Yeo, and R. Kwor, in *Semi-Insulating III-V Materials, Evian, 1982*, edited by S. S. Makram-Ebeid and B. Tuck (Shiva, Nantwich, 1982), p. 372.
- ¹⁵D. C. Look, *Phys. Rev. B* **24**, 5852 (1981).
- ¹⁶A. Chandra, C. E. C. Wood, D. W. Woodard, and L. F. Eastman, *Solid State Electron.* **22**, 645 (1979).
- ¹⁷H. J. Queisser and C. S. Fuller, *J. Appl. Phys.* **37**, 4895 (1966).
- ¹⁸J. W. Farmer and D. C. Look, *J. Appl. Phys.* **50**, 2970 (1979).
- ¹⁹J. Bernholc and S. T. Pantelides, *Phys. Rev. B* **18**, 1780 (1978).
- ²⁰A. Fazzio, J. R. Leite and M. L. DeSiqueira, *J. Phys. C* **12**, 3469 (1979).
- ²¹S. Das Sarma and A. Madhukar, *Phys. Rev. B* **24**, 2051 (1981).
- ²²N. P. L'in and V. G. Masterov, *Fiz. Tekh. Poluprovodn.* **10**, 836 (1976) [*Sov. Phys. Semicond.* **10**, 496 (1976)].
- ²³G. B. Bachelet, G. A. Baraff and M. Schluter, *Phys. Rev. B* **24**, 915 (1981).
- ²⁴M. Jaros and S. Brand, *Phys. Rev. B* **14**, 4494 (1976).
- ²⁵M. Jaros, *J. Phys. C* **8**, L550 (1975).
- ²⁶E. Louis and J. A. Verges, *Phys. Rev. B* **24**, 6020 (1981).
- ²⁷T. L. Reinecke and P. J. Lin-Chung, *Solid State Commun.* **40**, 285 (1981).
- ²⁸L. A. Hemstreet, *Phys. Rev. B* **22**, 4590 (1980).
- ²⁹D. V. Lang, in *Conference on Radiation Effects in Semiconductors, Dubrovnik, Yugoslavia, 1976*, edited by N. B. Urli and J. W. Corbett (Institute of Physics, London, 1977), p. 70.
- ³⁰O. F. Sankey and J. D. Dow, *Appl. Phys. Lett.* **38**, 685 (1981).
- ³¹G. D. Watkins, *Institute of Physics Conference Series No. 32* (Institute of Physics, London, 1977), p. 95.
- ³²O. F. Sankey and J. D. Dow, *Phys. Rev. B* **26**, 3243 (1982).
- ³³See, for example, A. G. Milnes, *Deep Impurities in Semiconductors* (Wiley, New York, 1973), p. 47.